Electronic Supplementary Material (ESI) for Nanoscale
This journal is © The Royal Society of Chemistry 2024

Supplementary Information

Friction-reduction effect of the hierarchical surface microstructure of carrion beetle by controlling the real contact area

Kazuma Tsujioka,[a] Yuji Hirai,[b] Masatsugu Shimomura[b,c] and Yasutaka Matsuo*[d]

[a]Graduate School of Chemical Sciences and Engineering, Hokkaido University, N13, W8, Kita-ku, Sapporo 060-8628, Japan.
[b]Graduate school of Science and Technology, Chitose Institute of Science and Technology, Bibi 758-65, Chitose, 066-8655, Japan.
[c]Department of Applied Chemistry and Bioscience, Chitose Institute of Science and Technology, Bibi758-65, Chitose, 066-8655, Japan.
[d]Nanotechnology Research Center, Research Institute for Electronic Science, Hokkaido University, N21W10, Kita-ku, Sapporo, 011- 0021, Japan.

E-mail: matsuo@es.hokudai.ac.jp;

Observation of the backside structure of the elytra.

Fig. S1 shows the field-emission scanning electron microscopy (FE-SEM) image of the backside of the elytra of *Necrophila japonica*. The front and back microstructures of the elytra differed greatly. The front side exhibited a hierarchical structure, with a wrinkled structure on top of a dome one, and only microtrichia were present on the back. The microtrichia may act as interlocks in the elytra, as reported in other papers [1-3]. The *Necrophila japonica* features flight muscle dimorphisms so that some individuals exhibit flight capability and flightlessness, although both groups exhibit fully developed wings [4, 5]. Therefore, microtrichia can exhibit an interlocking function, and individuals who have lost their flight capability may have microtrichia as a remnant of their ability to fly. More to the point, further research on interlocking structures, flight ability, and genetic factors may further elucidate the nature of the *Necrophila japonica*.

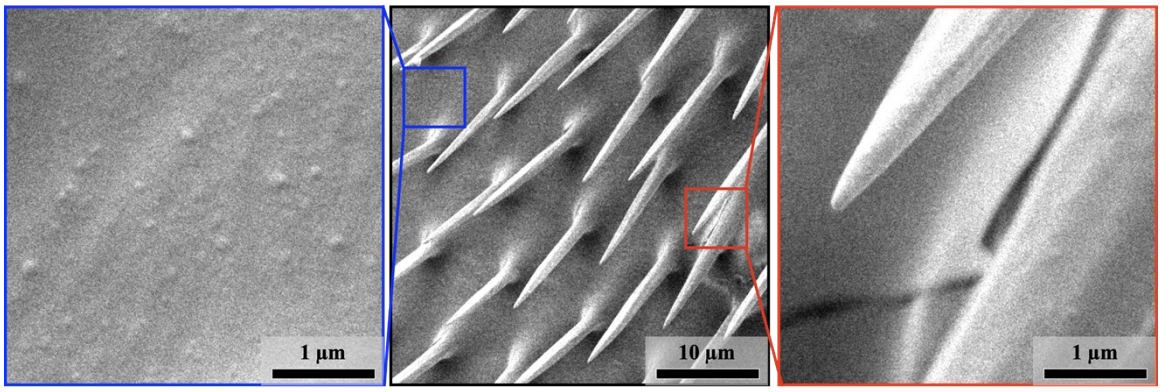

Figure S1. FE-SEM image of the back of the elytra of the carrion beetle. The images surrounded by blue (left), black (middle), and red (right) borders represent the magnified view of the microtrichia-free surface, the overall image, and the magnified view of the microtrichia, respectively.

Measurements of the water contact angle.

To investigate the microstructure functions of *Necrophila japonica*, 1 μL of water droplets was dropped onto the elytra surface, after which the static water contact angle (WCA) was measured. The contact angles were differentiated according to whether they were perpendicular or parallel to the wrinkle structure (Fig. S2(c)). The results are shown in Fig. S2(d). The WCAs were ~90°, displaying zero superhydrophobicity in either direction. Anisotropy was observed in different directions, with the WCA slightly higher in the perpendicular direction. Numerous studies have considered the anisotropy of static contact angle due to anisotropic microstructures [6-9]. According to these studies, the contact angle anisotropy is due to anisotropy in roughness. Put differently, WCA increases with Wenzel's law as the structure exists continuously and discontinuously in the parallel and perpendicular directions, respectively. The contact angle of the mimicked polystyrene (PSt) structure was higher than that of the flat surface without a structure (3 μL of water droplets), indicating that the mimicked structure exerted a water-repellent effect. However, the mimicked structure did not also exhibit superhydrophobicity.

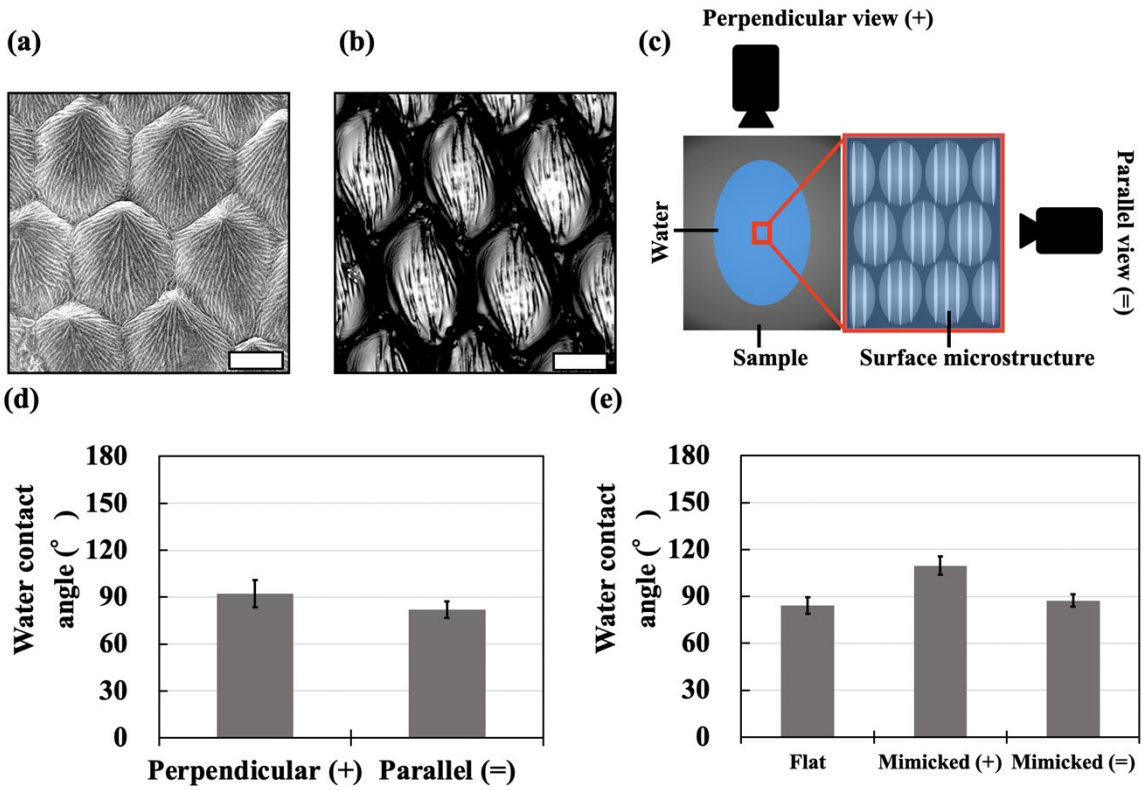

Figure S2. (a) FE-SEM image, (b) laser microscopy image, and (d, e) WCAs of the (a, d) carrion beetle elytra and (b, e) PSt carrion beetle elytra mimicked structure. For comparison, the WCA of a flat PSt surface was also measured. (c) Contact angle of the mimicked structure was divided into the perpendicular view (+) when observed from a direction perpendicular to the wrinkle structure and parallel view (=) when observed from a parallel direction. The white scale bar was 5 μm.

Electronic Supplementary Material (ESI) for Nanoscale.

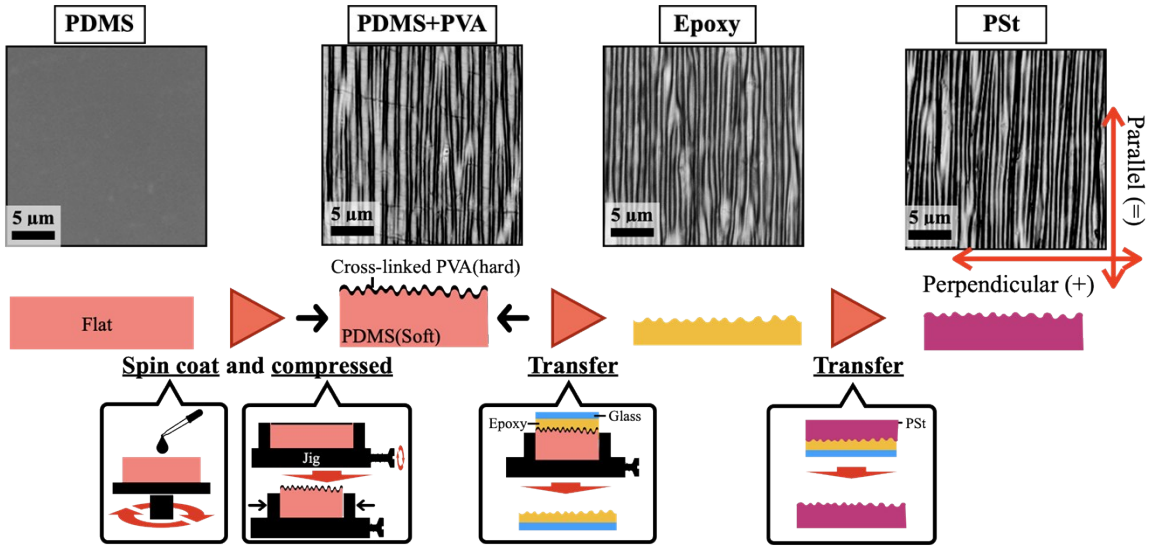

Figure S3. Preparation of the PSt wrinkle structures. The wrinkles were formed by preparing a hard polyvinyl alcohol (PVA) layer on soft polydimethylsiloxane (PDMS), followed by compression. The inset images are the laser microscopy images of each sample. The red arrow indicates the sliding direction.

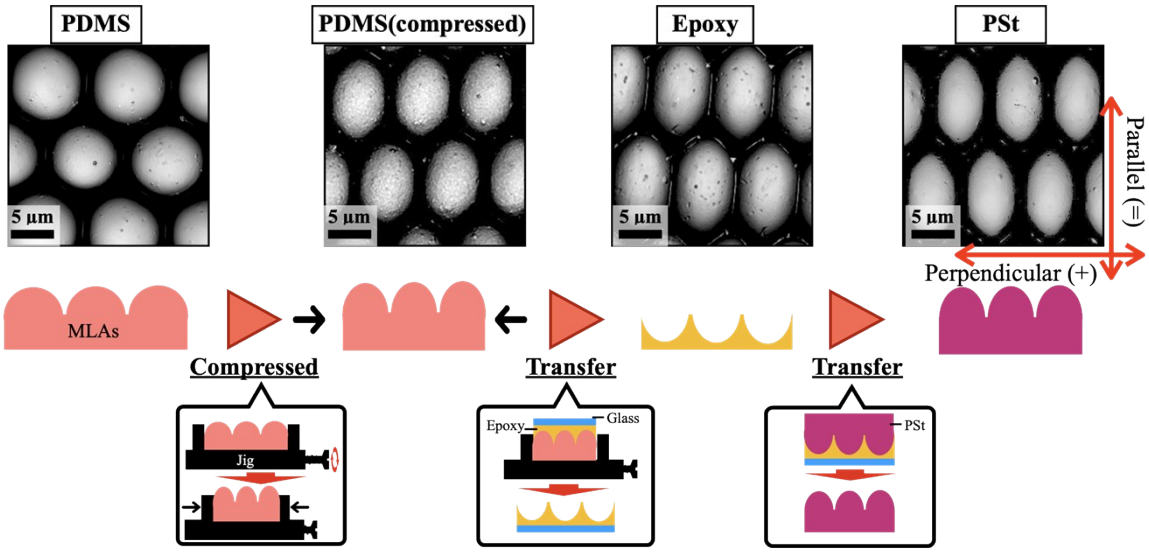

Figure S4. Preparation of the PSt microlens array (MLA) structures. The MLAs used for the measurements were formed by compressing PDMS-MLAs with circular structures. PVA was not spin-coated. The inset images are the laser microscopy images of each sample. The red arrow indicates the sliding direction.

Electronic Supplementary Material (ESI) for Nanoscale.

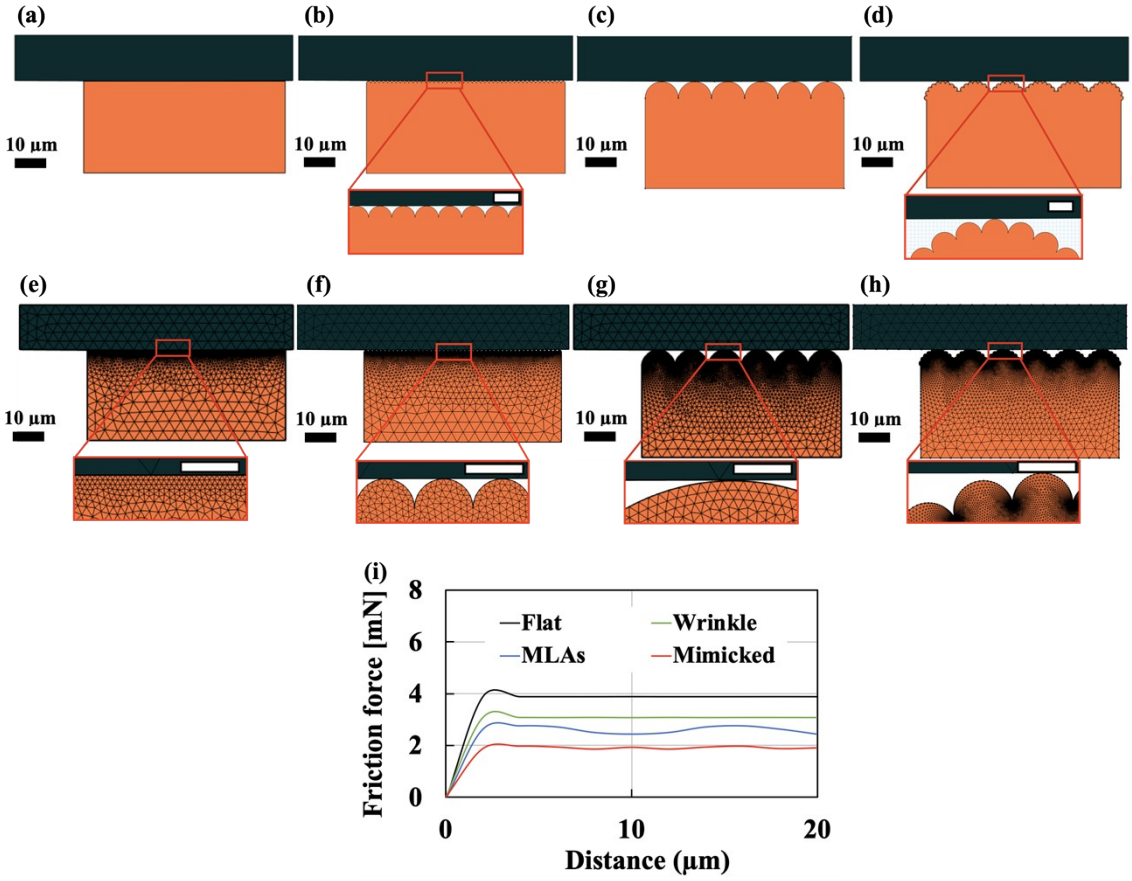

Figure S5. (a, b, c, d) Simulation and (e, f, g, h) meth models of (a, e) flat, (b, f) wrinkle, (c, g) MLA, (d, h) mimicked structures. The images with red borders represent the magnified views, and the scale bar is 1.4 µm. Only a portion of the indenter is shown. (i) the graph of calculation friction force vs sliding displacement curve.

The contact theory in the computational model follows the content described in the COMSOL Documentation, Contact Analysis Theory [10].

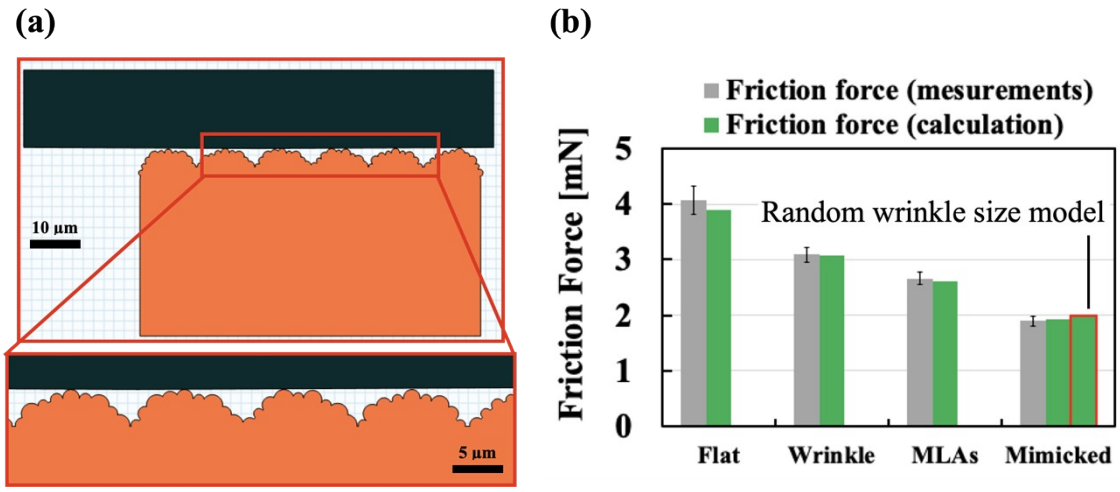

Figure S6. (a) Mimicked structure model with random wrinkle sizes and (b) calculation results.

The random mimicked structure model has wrinkles of random sizes in the range of 1-2 μm. The range of 1-2 μm is chosen because the measurement results of the wrinkle size at the top of the mimicked structure that was actually created were in the range of 1-2 μm. The calculation results were not significantly different from the actual measurement results and were within the error range. We believe that the slight difference is due to the difference in contact area caused by the difference in structure size.

SI References

1 J. Sun and B. Bhushan, *RSC Adv*, 2012, **2**, 12606–12623.

2 Gorb N. Stanislav, *Int J Insect Morphol Embryol*, 1998, **27**, 205–255.

3 J. Sun, C. Liu, B. Bhushan, W. Wu and J. Tong, *Beilstein Journal of Nanotechnology*, 2018, **9**, 812–823.

4 H. Ikeda and T. Sota, *Ecol Evol*, 2011, **1**, 97–105.

5 H. Ikeda, T. Kagaya, K. Kubota and T. Abe, *Evolution (N Y)*, 2008, **62**, 2065–2079.

6 J. Y. Chung, J. P. Youngblood and C. M. Stafford, *Soft Matter*, 2007, **3**, 1163–1169.

7 H. Yabu, Y. Nakamichi, Y. Hirai and M. Shimomura, *Physical Chemistry Chemical Physics*, 2011, **13**, 4877–4880.

8 S. Z. Wu, D. Wu, J. Yao, Q. D. Chen, J. N. Wang, L. G. Niu, H. H. Fang and H. B. Sun, *Langmuir*, 2010, **26**, 12012–12016.

9 D. Xia and S. R. J. Brueck, *Nano Lett*, 2008, **8**, 2819–2824.

10 COMSOL Documentation, Contact Analysis Theory https://doc.comsol.com/6.0/docserver/#!/com.comsol.help.sme/sme_ug_theory.06.73.html, (accessed October 2024)